ACS APPLIED MATERIALS & INTERFACES

Spotlight on Applications

www.acsami.org

Pyrolysis of Phenolic Impregnated Carbon Ablator (PICA)

Brody K. Bessire, Sridhar A. Lahankar, and Timothy K. Minton*

Department of Chemistry and Biochemistry, 103 Chemistry and Biochemistry Building, Montana State University, Bozeman, Montana 59717, United States

Supporting Information

ABSTRACT: Molar yields of the pyrolysis products of thermal protection systems (TPSs) are needed in order to improve high fidelity material response models. The volatile chemical species evolved during the pyrolysis of a TPS composite, phenolic impregnated carbon ablator (PICA), have been probed in situ by mass spectrometry in the temperature range 100 to 935 °C. The relative molar yields of the desorbing species as a function of temperature were derived by fitting the mass spectra, and the observed trends are interpreted in light of the results of earlier mechanistic studies on the pyrolysis of phenolic resins. The temperature-dependent product evolution was consistent with earlier descriptions of three stages of pyrolysis, with each stage corresponding to a temperature range. The two main products observed were H_2O and CO, with their maximum yields occurring at ~350 °C and ~450 °C, respectively. Other significant products were CH_4, CO_2, and phenol and its methylated derivatives; these products tended to desorb concurrently with H_2O and CO, over the range from about 200 to 600 °C. H_2 is presumed to be the main product, especially at the highest pyrolysis temperatures used, but the relative molar yield of H_2 was not quantified. The observation of a much higher yield of CO than CH_4 suggests the presence of significant hydroxyl group substitution on phenol prior to the synthesis of the phenolic resin used in PICA. The detection of CH_4 in combination with the methylated derivatives of phenol suggests that the phenol also has some degree of methyl substitution. The methodology developed is suitable for real-time measurements of PICA pyrolysis and should lend itself well to the validation of nonequilibrium models whose aim is to simulate the response of TPS materials during atmospheric entry of spacecraft.

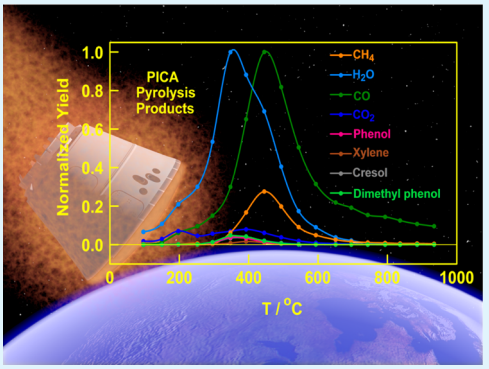

KEYWORDS: *pyrolysis, PICA, carbon/phenolic ablator, decomposition of phenolic*

1. INTRODUCTION

Thermal protection systems (TPSs) are required to shield spacecraft from the high temperatures generated in the stagnation region during atmospheric entry. TPSs can be designed to act as heat sinks, which use a material with a high heat capacity to absorb energy, or they can be designed to ablate and carry away thermal energy.[1,2] Composite ablative TPS systems are designed such that an organic resin matrix, surrounding a carbon fiber substrate, pyrolyzes to gaseous products and leaves a carbonaceous char behind. The gaseous products eventually make their way into the boundary layer and act as a transpirant, effectively cooling the leading edge of the spacecraft. The remaining char layer continues to absorb heat until it decomposes through sublimation or is removed by spallation.[3]

With the retirement of the Shuttle program and a renewed focus on Apollo-style spacecraft, research and development on carbon/phenolic ablative TPSs have gained renewed interest.[4−6] Several new phenolic-based rigid ablative TPSs, such as PhenCarb 28/15 (Applied Research Associates), BPA-FG (Boeing), and graded MonA (Lockheed), are being developed in order to facilitate the landing of heavy masses on Mars.[5] The heritage carbon/phenolic ablator, AVCOAT, will be used by NASA's Orion space capsule, but new variants of this material have been chosen for recent and future missions.[7] Phenolic Impregnated Carbon Ablator (PICA) is a state of the art carbon/phenolic ablator, which was developed at NASA Ames Research Center and which offers low mass per unit volume and high ablation performance.[8] PICA gained heritage during the successful re-entry of the Stardust sample return capsule as well as the recent successful entry, descent, and landing (EDL) of the Mars Science Laboratory (MSL) onto the surface of Mars.[9−12] A similar material, PICA-X, will be used on Space-X's commercial crew vehicle.[13]

At present, analysis and design of new ablative heat shields relies on material response models based on 50-year-old methodologies.[14,15] As a consequence, large uncertainties and margins are inherent in the design process, which leads to unnecessarily heavy heat shields and an inability to quantify the reliability of the resultant space hardware.[12] Building models that are based on fundamental understanding of the material behavior and validating them with high fidelity data will enable optimized risk and margin recommendations for a whole generation of future NASA and commercial space missions.

Received: November 8, 2014
Accepted: December 9, 2014
Published: December 9, 2014

DOI: 10.1021/am507816f
ACS Appl. Mater. Interfaces 2015, 7, 1383−1395

The current ablation models assume thermodynamic equilibrium chemistry to estimate the recession rate, and these models are known to be deficient because they over predicted the recession rate, for example, during the MSL entry into the Martian atmosphere.[16] Clearly, nonequilibrium chemistry is important in such environments; therefore, the new nonequilibrium models that are required must be founded on a fundamental understanding of the relevant nonequilibrium chemical kinetics and dynamics, which may be obtained from in situ measurements of dynamic chemical processes in real time. Chemical processes of relevance include the high-temperature decomposition of PICA-class materials and the interactions of decomposition products and boundary layer gases with each other and with the evolving ablator surfaces. Such detailed data will dramatically deepen our understanding of the processes occurring at the interface of a high-temperature hypersonic flow and an ablator, as well as provide a rigorous test of any new model that is developed. The work described herein is the first step in the development of a laboratory approach to understand the nonequilibrium ablation chemistry during atmospheric entry of carbon/phenolic composite TPS materials using advanced techniques that are well-established in the field of reaction dynamics but have not previously been applied to the understanding of the chemical processes in an atmospheric entry environment.

The work presented here builds on the substantial literature on the decomposition mechanisms of phenolic resins and carbon/phenolic composites at elevated temperatures. The phenolic polymers that have been studied are generally similar, but there can be important differences in the molecular structure that depend on the details of how the polymer was synthesized and cured. The resulting molecular structure can influence the decomposition mechanisms, including the identity and relative molar yields of pyrolysis products. The final structure of the cured polymer depends on the ratio of formaldehyde to phenol used as reagents, the type of catalyst used during synthesis, the cure time, the cure temperature, and the cure environment. Two types of phenolic resins, resoles and novolacs (Figure 1), may be synthesized by the reaction of phenol with formaldehyde. Resole resins are synthesized with an excess of formaldehyde and a basic catalyst. Novolacs are synthesized with an acidic catalyst and formaldehyde-to-phenol mole ratio of less than one, and they require a cross-linking agent (hexamethylenetetramine).[17] In general, the structure of a cured phenolic resin consists of a three-dimensional network of phenol molecules joined together by methylene cross-links. Earlier studies suggest that dibenzyl ether cross-links are formed in resole resins during the curing stage and that methylol groups may also remain after curing, which may affect the process of thermal degradation.[18,19] Jackson and Conley suggested that oxygen in the polymer structure plays a significant role in the degradation of resole-type resins,[18] in contrast to the conclusions from a study performed by Moterra and Low,[19] who reported that such incorporated oxygen does not play a significant role in the thermal degradation of novolac-type resins. Ouchi and Honda performed a study in which the pyrolysis products of seven different phenolic resins were analyzed by mass spectrometry.[20] The resins were synthesized with varying amounts of substitution by hydroxyl and methyl groups on phenol; their structures prior to synthesis are illustrated in Table 1. Ouchi and Honda reported that there

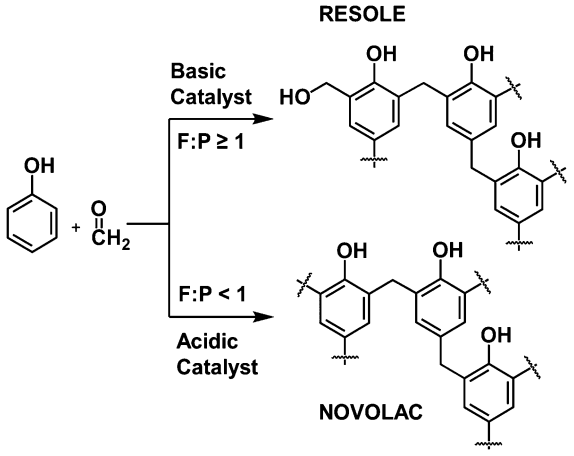

Figure 1. General synthesis of resole and novolac phenolic resins.

Table 1. Relationship between Phenol Precursor Structure, Formaldehyde:Phenol Ratio, Catalyst, and the Relative Yields of CO and CH_4 during Pyrolysis of the Corresponding Phenolic Resin[a]

Precursor	Formaldehyde : Phenol	Catalyst	CO : CH_4
	1	NH_4OH	0.9 : 1.0
	1	HCl	0.6 : 1.0
	2	NH_4OH	0.6 : 1.0
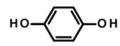	1	NH_4OH	3.0 : 1.0
	1	NH_4OH	12.0 : 1.0
	1	NH_4OH	1.0 : 2.0
	1	NH_4OH	1.0 : 6.0

[a]Based on the results of Ouchi and Honda.[20].

is a direct relationship between the identity of each phenol molecule used to synthesize the resin and the relative molar yields of products that were evolved during pyrolysis. For example, a key result was that the molar ratio of CO to CH_4 increased with increasing hydroxyl substitution in the molecular structure, whereas this ratio decreased with increasing methyl substitution (see Table 1). Thus, the nature of the phenolic resin—resole vs novolac—as well as the functional group substitution on the phenol rings in the polymer (resulting either from the synthesis or the cure environment) will likely affect the decomposition mechanisms and the observed relative yields of gaseous pyrolysis products.

Previous work on the pyrolysis mechanisms of phenolic resins has revealed three overlapping stages of pyrolysis.[18,20−22] A schematic representation of the stages of pyrolysis is presented in Figure 2. As the resin is heated from ambient, there is outgassing of the resin as absorbed gases are released

DOI: 10.1021/am507816f
ACS Appl. Mater. Interfaces 2015, 7, 1383−1395

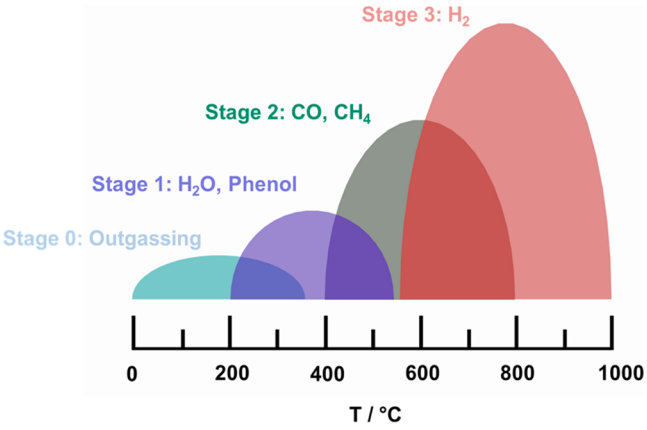

Figure 2. Three overlapping, temperature-dependent stages of phenolic pyrolysis, labeled with the corresponding major gas-phase pyrolysis products. Stage 1 (blue) spans an approximate temperature range of 200−550 °C. Stage 2 (green) spans the range 400−800 °C. Stage 3 (red) corresponds to temperatures above 560 °C. Absorbed gases may escape from the material during the earliest stage of heating (Stage 0: Outgassing).

(labeled "Stage 0" in Figure 2). The first stage of pyrolysis occurs when the temperature is elevated sufficiently ($T \approx 200-550$ °C) such that the phenolic resin depolymerizes and produces phenol and its methyl substituted derivatives. In addition to depolymerization, cross-linking of the phenolic backbone takes place between hydroxyl or methylol functional groups, as evidenced by the evolution of H_2O.[18,20] Another product, as shown in the results reported here, is CO, which is produced in relatively low yields in the first stage of pyrolysis. During the second stage of pyrolysis ($T \approx 400-800$ °C), bonds created from the previous cross-linking events are broken, leading to the evolution of H_2, CO, and CH_4.[18,20,21] H_2 is the dominant product evolved during the third stage of pyrolysis ($T \approx 560-1000$ °C) as aromatic rings fuse to form a carbonaceous char.[20,21]

Although the general pyrolysis behavior of phenolic resins has been gleaned from previous studies, these studies disagree on the specific steps involved in the decomposition. The contradictions have been discussed in detail by Trick and Saliba[22] and are summarized here. Experiments performed by Ouchi and Honda[20] and similar work done later by Jackson and Conley[18] have led to opposing explanations for the early evolution of water (Stage 1, $T \approx 200-550$ °C). In the mechanism proposed by Ouchi and Honda, a condensation reaction takes place between the phenol groups of the polymer to form a diphenyl ether bond. On the other hand, Jackson and Conley suggest that methylol groups that are attached to phenol undergo a condensation reaction that results in methylene cross-links. Jackson and Conley further propose that ether cross-links are not formed at these temperatures. Parker and Winkler[21] propose that H_2O evolves as a consequence of the decomposition of ether linkages but only during the latter stages of pyrolysis ($T \approx 700-800$ °C). Parker and Winkler also suggest that phenol polymer units that have multiple bonds to adjacent phenol groups are retained in the polymer and that any observed phenol or cresol products are the result of the decomposition of pendant phenol groups.[21] During the cross-linking stage of pyrolysis (Stage 2, $T \approx 400-800$ °C), Parker and Winkler, as well as Jackson and Conley, suggest that the evolution of CO is a direct consequence of the decomposition of carbonyl cross-links that have been formed previously. Originally, Ouchi and Honda suggested that CO evolves as a result of the decomposition of ether groups formed from condensation reactions that occur in the first stage of pyrolysis. However, in a later study Ouchi revised the pyrolysis mechanism to include carbonyl functional groups as a source of CO, following the observation of infrared absorption bands at 1660 cm^{-1} to 1630 cm^{-1}.[23] Ouchi and Honda[20] and Parker and Winkler[21] predicted H_2 as the dominant species evolved toward the end of pyrolysis, with H_2 coming from aromatic rings as they become carbonized. Jackson and Conley,[18] however, did not predict the evolution of H_2 at any point during the process of thermal degradation.

In a somewhat more recent qualitative study, Trick and Saliba[22] collected infrared spectra of the material remaining after the pyrolysis of a carbon fiber/phenolic composite, and they drew many of the same conclusions as Ouchi and Honda,[20] Parker and Winkler,[21] and Jackson and Conley,[18] as well as some new conclusions that contradicted the previous studies. For instance, Trick and Saliba[22] proposed a one-step mechanism for the evolution of CH_4, in contradiction to the two step mechanism that was proposed by Ouchi.[23] Trick and Saliba[22] also suggested that that there is little evidence to support carbonyl formation even though they detected a very weak signal for a carbonyl stretch at 1658 cm^{-1} On the other hand, Jackson and Conley[18] and Ouchi[23] unequivocally suggested the formation of carbonyl functional groups in the decomposing phenolic polymer. The discrepancies in the reported qualitative thermal degradation mechanisms of phenolic resins need to be resolved to enhance our basic understanding and validate emerging models designed to predict quantitative yields of pyrolysis products. This resolution and the consequent model validation may come from reliable measurements of the quantitative yields from a material whose thermal degradation is the focus of model simulations.

Quantitative yields have been reported for the pyrolysis of various phenolic-based materials, although questions remain about the accuracy of the results. The majority of such studies were conducted during the development of the Apollo spacecraft,[20,24−26] and there have also been more recent studies during the last two decades.[27−29] The most common techniques employed in the 1960s were mass spectrometry (MS) as well as gas chromatography (GC). More recent efforts have implemented modern versions of GC and MS, as well as the combination of the two (GC-MS). As mentioned above, Ouchi and Honda performed an experiment in which the thermal decomposition mechanisms of several different phenolic resins were studied (in steps of approximately 100 °C) using mass spectrometry.[20] Although this work was helpful in demonstrating the relationship between the reagents used during synthesis and the relative yields of pyrolysis products, the manner in which the products were collected and analyzed was subject to significant errors. After the resin was pyrolyzed, the gaseous products were collected and stored in a reservoir at a relatively high pressure (50 Torr) until pyrolysis was complete, thus providing the opportunity for secondary reactions to occur. In addition, analysis of the pyrolysis products was incomplete. While the permanent gases were analyzed by MS, H_2O and other condensable products were trapped on a coldfinger. H_2O was measured by gravimetric methods and the remaining products were weighed and defined as "lower molecular mass substances," which presumably were a mixture of phenol and substituted phenols. There were

DOI: 10.1021/am507816f
ACS Appl. Mater. Interfaces 2015, 7, 1383−1395

potential errors in other studies as well. Friedman performed an experiment in which a phenol-formaldehyde sample was quickly pyrolyzed with a flash lamp, and the decomposition products were subsequently analyzed with the use of a time-of-flight mass spectrometer.[24] Direct temperature measurements of the sample were not made, and the measurements of decomposition products were limited to time intervals of 30 min because of the slow pumping speed of the reaction chamber. Shulman and Lochte performed a pyrolysis experiment on two resole phenolic resins using the MS thermal analysis method (MTA).[25] The MTA method is implemented by heating a sample in a furnace that is located directly beneath an electron beam. As the resin is heated, pyrolysis products are immediately ionized and subsequently analyzed in a time-of-flight mass analyzer. Shulman and Lochte reported day to day variations in sensitivity and instrumental settings, resulting in measurements with limited absolute accuracy. Quantitative analysis using GC as an analytical technique was performed on a novolac resin by Sykes.[26] In order to analyze all of the pyrolysis species evolved from the resin, three different columns were used in separate experiments in order to characterize H_2O, noncondensable gases, and aromatic hydrocarbons, respectively. The use of three GC columns made it difficult to obtain accurate relative yields of products that were analyzed with different columns. In a recent effort to obtain more accurate quantitative data, Wong et al. performed a pyrolysis experiment using a batch reactor.[27] They loaded a phenolic resole sample into a quartz tube, which was then placed inside a ceramic furnace. The sample was pyrolyzed while the furnace was set to a specific temperature and held for 1 h to ensure complete degradation of the material. Permanent-gas products from pyrolysis were analyzed by GC, and products that are liquids at room temperature were trapped in a condenser for analysis at a later time. Again, the possibility of secondary reactions exists, and perhaps more importantly, the batch-reactor approach does not lend itself well to nonequilibrium measurements of evolving products in real time. On the other hand, the approach of Wong et al. allows for mass balance, including the determination of the masses of the gaseous products and the total mass loss of the sample, after the pyrolysis of the sample has been quenched by lowering its temperature.

Several of the more modern studies have combined GC with MS in order to quantify the molar yields of pyrolysis products, but they, too, were incomplete or subject to inaccuracies. Sobera and Hepter[28] used GC-MS to pyrolyze novolac and resole phenolic resins, but their experiments were limited to temperatures of 650, 770, and 900 °C. Although yields of volatile organic pyrolysis products were reported (benzene, phenol, cresol, etc.), Sobera and Hepter did not report yields of permanent gases (H_2, CO, CO_2, etc.) that are known to dominate at the temperatures used in their study. In another recent study, Bennett et al. used a combination of GC, MS, and infrared spectroscopic techniques in order to measure total quantitative yields of pyrolysis products from a phenolic resole resin over a large temperature range (intervals of 100 °C from 100 to 800 °C).[29] A pyroprobe (CDS 5200 pyrolyzer) was coupled to a GC-MS system to measure organic products, and yields of permanent gases were measured by coupling the pyroprobe to a Fourier transform infrared (FTIR) spectrometer. Even though both organics and permanent gases were measured, yields of H_2 were not quantified. Ultimately, Bennett et al. reported inconsistencies in the data and suggested that more consistent data would be gathered when one sample is analyzed with two analytical techniques simultaneously. Bennett et al. also suggested that another method, such as GC coupled to thermal conductivity detection, would be needed in order to detect H_2.

Shortcomings of each of the previous studies have resulted in uncertain quantitative yields of pyrolysis products. In fact, there has not been a study in which a single technique has been used to measure the quantitative yields of the complete range of pyrolysis products as a function of time over the full range of temperatures that covers all three pyrolysis stages. The uncertainties in the measurements are compounded by the unknown differences in the decomposition mechanisms for the different types of phenolic samples in each study, leading to the current situation where there is not a "go-to" set of data that can be used for the validation of new models aimed at predicting the thermal degradation of carbon/phenolic ablators, such as PICA, that have been chosen for use in actual space missions.

Mass spectral measurements taken in situ provide an excellent way to obtain accurate and precise data for the whole range of pyrolysis products, and they are well-suited for probing the time-dependent decomposition mechanisms of materials under controlled heating conditions. A key objective of the work described herein was therefore to develop the methodology to measure relative molar yields of pyrolysis products under conditions where (1) time and temperature are independent variables and (2) there is no interaction of products with each other, with the hot sample surface, or with any container walls after they leave the decomposing material. A second important objective was to improve our understanding of the decomposition mechanisms of the specific carbon/phenolic composite, PICA, as this material has been chosen for several NASA missions and is an important model material for ongoing theoretical efforts to describe the in-depth temperature response of ablative TPS materials. Our approach was to use a mass spectrometer to detect the pyrolysis products in situ as they desorbed from a PICA sample that was heated in high vacuum and to determine relative molar yields of the products by a validated interpretation of the mass spectral data.

2. EXPERIMENTAL METHODS

The experiments utilized a crossed molecular beams apparatus with a rotatable mass spectrometer detector.[30−32] For the experiments described here, a heated PICA sample was placed in front of the detector in vacuum, and mass spectra of pyrolysis products were collected as the temperature of the sample was increased. Figure 3 shows a diagram of the experimental setup. A fitting method was developed to derive relative molar product yields from the mass spectral data.

The samples were heated by passing current through them. The sample mount (Figure 4) consists of two water-cooled copper blocks that are electrically isolated by a ceramic spacer and connected to a TDK-Lambda GEN 30−25 power supply. Current flowed through copper cooling tubes. Cooling water was circulated through the mount by a pair of chillers, each held at a temperature of 25 °C.

PICA samples were obtained from Fiber Materials Inc. Each sample in this study was cut to the dimensions of 25 mm long × 6 mm wide × 5 mm thick. A K-type thermocouple was attached to the center of the back side of the PICA sample during each experimental run in order to obtain precise temperature measurements. Before each experimental run, a fresh PICA sample was mounted, and the vacuum chamber was pumped out overnight to a base pressure in the low 1×10^{-7} Torr range.

The mass spectrometer is triply differentially pumped (Figure 3), in order to ensure an extremely low pressure ($<1 \times 10^{-11}$ Torr) in the

DOI: 10.1021/am507816f
ACS Appl. Mater. Interfaces 2015, 7, 1383−1395

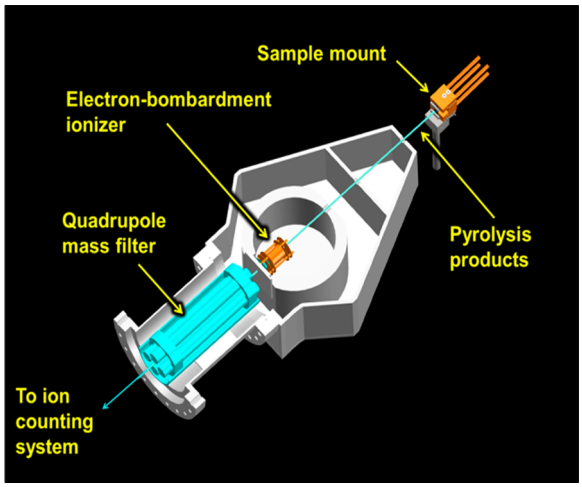

Figure 3. Schematic diagram of the experimental setup, where the resistively heated PICA sample is placed in a separate vacuum chamber in front of a triply differentially pumped mass spectrometer detector with an electron-impact ionizer, a quadrupole mass filter, and a Daly type ion counter. Volatile products desorb from the sample in all directions, but only those products that exit the surface from a roughly 3 mm × 3 mm square area of the surface pass through the apertures of the detector and reach the ionizer.

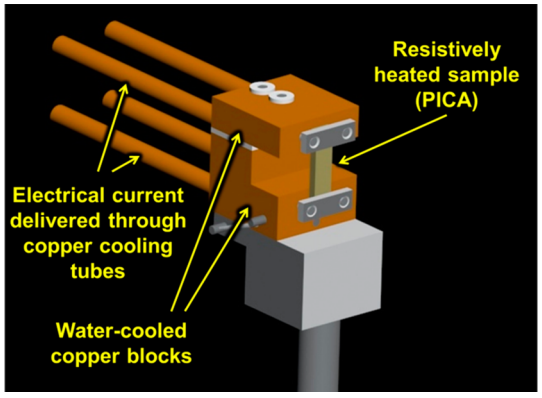

Figure 4. Mount used to heat PICA samples. The top and bottom copper blocks act as electrodes and are separated by a ceramic spacer and cooled with water that flows through copper tubes attached to the back. The copper tubes also carry the electrical current used to heat the sample restively.

ionization region and therefore low background and high detection sensitivity. Pyrolysis products emerge continuously from the heated sample and pass through three apertures and then enter the electron-impact (EI) ionizer. Ions are focused into a quadrupole mass filter, and the mass-selected ions are converted into electrical pulses by a Daly type ion counter.[32] The mass-to-charge ratio (m/z) accepted by the quadrupole is varied with time by control electronics, and the ion signal (which is proportional to number density) as a function of time is accumulated with a multichannel scaler. The m/z accepted by the mass filter as a function of time allows the data accumulated with the multichannel scaler to be converted into a mass spectrum, which is number density as a function of m/z ratio. The products that are not ionized pass through the ionization region and enter a different region of differential pumping, thus ensuring that any products that scatter from surfaces in the detector cannot re-enter the ionizer and have a second chance to be ionized. Details of the mass spectrometer detector have been described previously.[32]

Samples were heated initially from room temperature to 100 °C within a matter of seconds, and then they were heated to nearly 950 °C in roughly 50 °C steps, with a hold time of 15−20 min at each temperature step. Mass spectra were collected at specific times after each heating increment. Associated with each heating increment was a pressure jump in the vacuum chamber, as pyrolysis products desorbed quickly from the sample. The high flux of gases desorbing from the sample immediately after each heating increment saturated the detector, so a gate valve that isolates the mass spectrometer detector from the sample chamber was closed during the initial moments of each heating increment and then opened later for data collection. Figure 5 shows an example of the partial pressure change in the sample

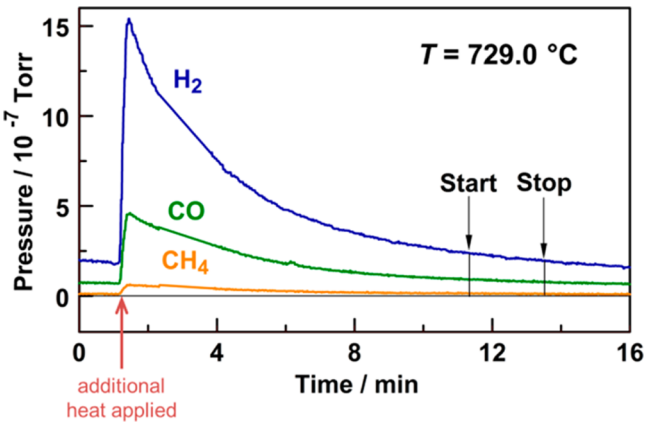

Figure 5. Partial pressure of H_2, CO, and CH_4 in the sample chamber as a function of time after a PICA sample was raised (starting at 1.5 min from an arbitrary time zero) from 686.6 to 729.0 °C, measured with a residual gas analyzer (RGA). Five mass spectra were collected consecutively during the time from "Start" to "Stop", and these mass spectra were summed to give the mass spectrum corresponding to a temperature of 729.0 °C. Hydrogen was clearly detected by the RGA, even though it was not monitored during the collection of mass spectra with the detector depicted in Figure 3.

chamber for three pyrolysis products, H_2, CO, and CH_4, after a sample was heated from 686.6 to 729.0 °C. Data for this figure were collected with a residual gas analyzer (RGA) in the sample chamber. After the heating current was increased, the temperature of the sample rose to its final value within seconds, and the partial pressure of pyrolysis gases rose quickly to a maximum and then decayed at a relatively slow rate, on the time scale of minutes. In general, after the pressure in the sample chamber had decreased to an acceptable level (~6×10^{-7} Torr), mass spectra were collected repeatedly (with 30 s being required to collect a mass spectrum). After the difference in intensity between two successive spectra had decreased to less than 20%, a set of five mass spectra were collected and summed. Thus, data for a particular temperature were typically collected during a 2.5 min period in the range of 12−15 min after each temperature step. The typical range over which mass spectra were collected after a temperature step is illustrated in Figure 5. The pyrolysis products were thus monitored essentially after a steady state had been reached at a given temperature. Each individual mass spectrum was collected by scanning m/z values in steps of 0.045 amu, with a dwell time of 10 ms at each step. The summed spectrum collected at each temperature was used to determine the relative molar yields of pyrolysis products using a procedure, described in the next section, that involved fitting the summed mass spectrum. Similar temperature-dependent mass spectral data were collected for four different samples, and the results were averaged.

3. RESULTS AND ANALYSIS

A. Analysis of Mass Spectra. The relative molar yield of each detected species at a given sample temperature was derived from the mass spectrum collected at that temperature. The relative molar yields are equivalent to the relative fluxes of the products that desorb from the sample. All products exit the

DOI: 10.1021/am507816f
ACS Appl. Mater. Interfaces 2015, 7, 1383−1395

Table 2. List of Compounds Selected As Potential Pyrolysis Products and Their Respective Electron-Impact Ionization Cross-Sections[a]

Product Species	Ionization Cross Section / Å^2	Product Species	Ionization Cross Section / Å^2
CH_4	3.52	o-cresol	17.19
H_2O	2.28	p-cresol	18.94
CO	2.52	mesitylene	18.18
CH_2CH_2	5.12	2,6-dimethyl phenol	19.82
CH_3CH_3	6.42	2,4-dimethyl phenol	21.58
CH_3OH	5.11	3,4-dimethyl phenol	23.82
Ar	2.99	2,4,6-trimethyl phenol	24.22
CO_2	3.52	hexamethylenetetramine	-
$CH_3CH_2CH_3$	8.62	2-methylnapthalene	22.12
$(CH_3)_2CHOH$	10.94	2-methyl-1,1'-biphenyl	25.58
benzene	15.03	dibenzofuran	33.05
hexane	16.58	diphenyl methane	34.18
2,2-dimethyl-propanol-1-ol	-	diphenyl ether	34.18
toluene	16.62	anthracene	33.05
phenol	14.55	benzophenone	29.54
o-xylene	15.81	xanthene	33.05
p-xylene	17.04	(4-methylphenyl)-phenyl-methanone	32.56

[a]Of the 34 compounds listed, only 14 (shown in color and larger font) made a significant contribution to the fit of the experimental mass spectra. The total EI ionization cross-sections were taken from several sources[35−37] and scaled to give a set of cross-sections that were consistent with those reported in the NIST database.[38] Electron-impact ionization cross sections for 2,2-dimethyl-propanol-1-ol and hexamethylenetetramine were not found in the literature, so the relative molar yields for these species were not corrected for ionization cross section. The lack of correction for ionization cross section would lead to an overestimate of the relative molar yield, but even without correction, the yields of these two species were negligible.

surface in thermal equilibrium, and their fluxes emanating from a given point on the surface should therefore have a cosine angular distribution about the surface normal. When the angular distributions of the products are the same, the relative flux integrated over all exit angles can be obtained from the flux measured at one exit angle. Thus, all products were collected with the mass spectrometer oriented along the surface normal. Although the EI ionizer makes the mass spectrometer a number density detector, it is a simple matter to convert the measured signals to relative flux.[33]

A list of 34 compounds that might be produced from PICA pyrolysis was generated from observations of pyrolysis products that have been reported in the literature on the pyrolysis of the neat phenolic resins, as well as composite materials made with similar resins. Table 2 lists all of the compounds that were used to construct the list. All compounds on the list are stable, as it was assumed that any radical species that might have been produced initially had ample time to react (for example, by abstracting a hydrogen atom) and form a stable species while following a tortuous path through the decomposing polymer and incipient char layer. H_2 is undoubtedly among the pyrolysis products, but it was not included in the list of potential products because our mass spectral range at the time the data were collected did not include m/z ratios less than 10.

The calculation of relative molar yields required the knowledge of the EI ionization mass spectra for the compounds on the list in Table 2, which were taken from the National Institute of Standards and Technology (NIST) database.[34] The first step in the calculation of the relative molar yield of each molecular species was to fit every peak in its NIST reference mass spectrum with a Gaussian function representative of the mass resolution of our mass spectrometer (~1 amu). Next, linear combinations of the Gaussian-fit mass spectra for individual species were fit to an experimental mass spectrum. Figures 6 and 7 display representative mass spectra that were collected at relatively low and high temperatures, respectively. The raw data, with background subtracted, are indicated by the green dots, and the fits are indicated by the solid blue lines. Each fit was optimized by minimizing the residuals. Relative molar yields were obtained from the coefficients in the linear

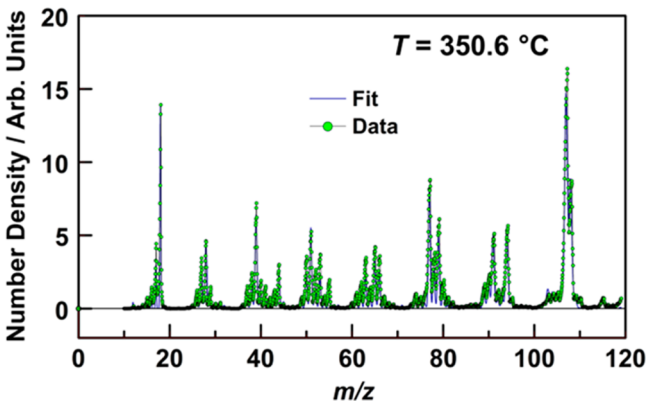

Figure 6. Representative mass spectrum and associated fit of pyrolysis products detected with a PICA sample temperature of 350.6 °C. The small peak at m/z = 115 suggests that a diphenyl ether group might be evolved at this temperature.

DOI: 10.1021/am507816f
ACS Appl. Mater. Interfaces 2015, 7, 1383−1395

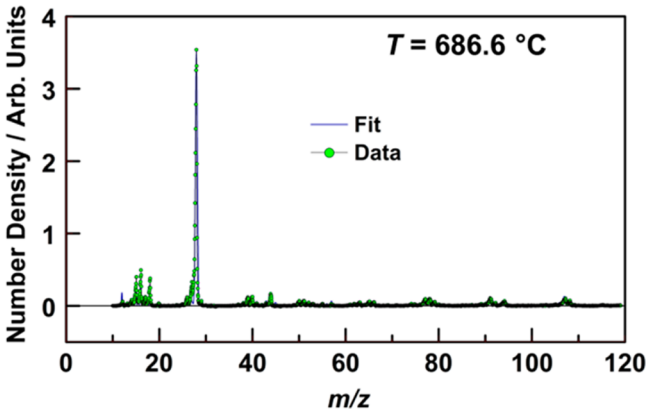

Figure 7. Representative mass spectrum and associated fit of pyrolysis products detected with a PICA sample temperature of 686.6 °C. CO and CH_4 dominate the spectrum at this temperature, as cross-links are broken and the material is reduced to a char.

combination that gave the best fit to the experimental mass spectrum by weighting each coefficient by the total EI ionization cross-section for the respective chemical species and then dividing the result by the square root of the molecular mass of the species to obtain flux.[33] The total EI ionization cross sections were taken from several sources[35−37] and scaled to give a set of cross-sections that were consistent with those reported in the NIST database.[38] The values that were used to determine the relative molar yields reported here are listed in Table 2.

There are some key assumptions in the analysis that add much uncertainty to the relative molar yields. Implicit in the analysis that was done is the assumption that the fragmentation patterns of the compounds in the NIST database are identical to those for our mass spectrometer. We have not conducted a systematic study of fragmentation patters of all the compounds listed in Table 2, but we have verified that the fragmentation patterns of phenol and *o*-cresol measured in our mass spectrometer are similar to those in the NIST database. Another assumption in the analysis is that the transmission probability of ions through the quadrupole mass filter is constant over the m/z range in our experiments. The transmission function probably favors higher-mass products in our experiments,[33] in which case the relative molar yields of the higher-mass products that we observed (e.g., phenol and its methylated derivatives) would actually be lower than what we report. The uncertainties associated with these assumptions are difficult to estimate. Nevertheless, our reported relative molar yields can be considered to be qualitatively, and even semiquantitatively, correct. Work is underway to determine the transmission function of our mass filter and build our own database of fragmentation patterns for the possible pyrolysis products, in anticipation of future experiments where the temperature-dependent relative molar yields of the products will be measured under nonequilibrium conditions in real time.

B. Relative Molar Yields. Of the 34 species chosen as potential gas-phase products for fitting the mass spectra, only 14 species consistently contributed significantly to the fits. A table of the 14 species, with their relative molar yields at each pyrolysis temperature, is presented in Supporting Information. Most of the molecules that have been included in the list shown in Table 2 were chosen because they have been suggested as decomposition products in prior literature. The four molecules, hexamethylenetetramine, hexane, isopropanol, and methanol, where chosen because they are commonly used as solvents during the synthesis of phenolic resins. The inclusion of these molecules and Ar improved the fit of the mass spectra at low temperatures, but their relative molar yields quickly vanished at temperatures exceeding 200 °C. The appearance of Ar among the desorbed products at low temperatures suggests that it must have been trapped in the polymer, but the source of Ar is unknown and we can only speculate that an Ar-rich atmosphere might have been used during the processing of the PICA composite. The possible decomposition product, diphenyl ether, has a parent mass (m/z = 170) that is above the mass range used, and we could only obtain good fits to the mass spectra by considering possible daughter fragments from diphenyl ether. The small peak in the mass spectrum at m/z = 115, which corresponds with a daughter fragment of diphenyl ether, supports the assumption that diphenyl ether might be a minor product. But the very low yield of this assumed product and the lack of detection of its parent mass do not give us sufficient confidence to report diphenyl ether as a significant pyrolysis product. Three of the species that were detected, xylene, cresol, and dimethyl phenol, may have different isomeric structures, but the differences in the fragmentation patterns of the isomers of these species are not sufficient to allow their distinction in our mass spectrometer. For example, *o*-xylene and *p*-xylene have maxima in their mass spectra at the same daughter mass of m/z = 91. Relative to this largest peak, both isomers have parent and daughter peaks of very similar magnitudes at m/z = 106 (parent), 77, 65, and 39. Because of the indistinguishability of the isomers by our mass spectrometer, the molar yields reported for xylene, cresol, and dimethyl phenol include all the isomers of the respective species. Neglecting Ar, diphenyl ether, and the four solvent species mentioned above, and grouping the isomers of detected species, the focus of the results is on eight significant species that were detected during the pyrolysis of PICA: H_2O, CH_4, CO, CO_2, phenol, xylene, cresol, and dimethyl phenol.

Figure 8 shows a plot of the relative molar yields of the species mentioned above as a function of pyrolysis temperature. The relative molar yields are plotted as the observed yield relative to the maximum yield which came from CO at 444.8 °C. The detected lower-mass pyrolysis products were H_2O, CH_4, CO, and CO_2, whereas the higher-mass (aromatic) products were xylene, phenol, cresol, and dimethyl phenol.

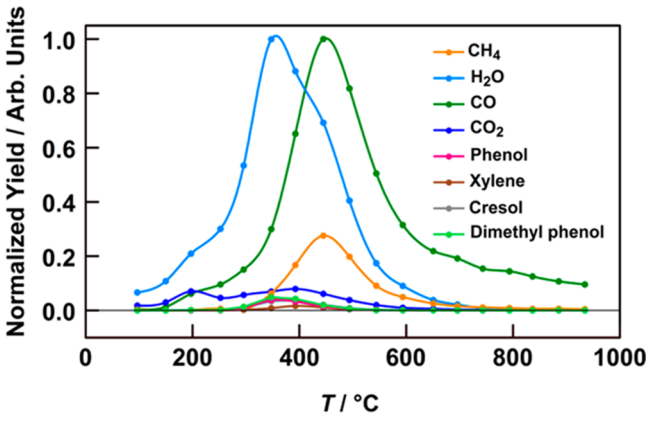

Figure 8. Normalized yields of gaseous pyrolysis products as a function of PICA temperature. The yield of each species at each temperature has been normalized to the yield of CO at 444.8 °C.

DOI: 10.1021/am507816f
ACS Appl. Mater. Interfaces 2015, 7, 1383−1395

H_2O and CO were the dominant products that were detected over the temperature range in this study, with H_2O being the dominant product below ~400 °C. The yield of CO_2 rises up at 150 °C where it levels off until about 400 °C and then begins to drop, disappearing completely near 650 °C. CH_4 begins to evolve around 300 °C and its yield reaches a maximum near 450 °C. All the higher-mass products evolve from 300 to 450 °C and have maxima in their yields between 350 and 400 °C. The higher-mass products have much lower relative molar yields than the lower-mass products.

C. Test of Analysis Procedure with a Binary Mixture. The methodology used to derive relative molar yields from the mass spectra was tested with the use of a binary mixture of phenol and *o*-cresol. A vessel containing these two liquids (purchased with a stated purity of 99% from Sigma-Aldrich) with known mole fractions of 0.54 and 0.46, respectively, was immersed in a temperature-controlled ethanol bath, and the vapor from the mixture at a given temperature was expanded through an effusive nozzle and interrogated with the mass spectrometer detector. Mass spectra of the vapor were collected with the liquid mixture at different temperatures, starting at 20 °C and reduced in 5 °C increments down to 0 °C. A representative mass spectrum collected at 20 °C and the corresponding optimized fit are shown in Figure 9. In general, the mass spectrum is fit well using the procedure discussed above.

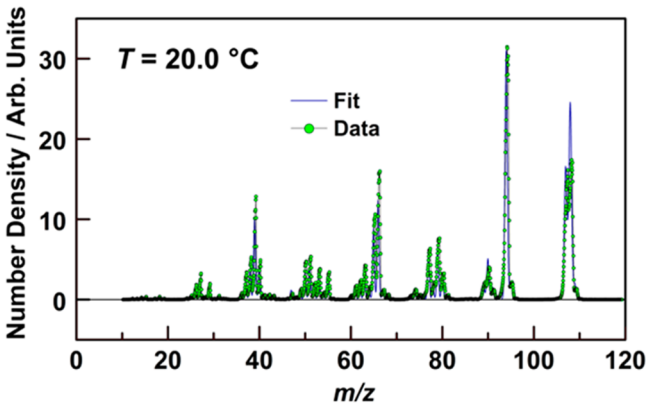

Figure 9. Mass spectrum of the vapor from a binary mixture of phenol and *o*-cresol (with mole fractions of 0.54 and 0.46, respectively) that was held at 20 °C. The raw data are represented by the green dots and the blue line represent the fit using the procedure described in the text.

The accuracy of the procedure was validated by comparing the known partial pressure ratio in the vapor to the partial pressure ratio derived from the mass spectra. The known partial pressure ratio in the vapor comes from the finding of Rhodes et al. that phenol and *o*-cresol form an ideal solution.[39] The vapor pressure of the pure substance for each species in the binary mixture was calculated from the integrated Clausius−Clapyeron equation, whose parameters are available in the literature.[40] According to Raoult's Law, the vapor pressure for each pure substance was multiplied by its corresponding mole fraction in the liquid mixture to yield the partial pressure of each constituent at each temperature in the experiment. Figure 10 shows a comparison between the calculated partial pressure ratios of phenol to *o*-cresol at different temperatures and the partial pressure ratios that were derived by fitting the mass spectra using the same methodology that was described in

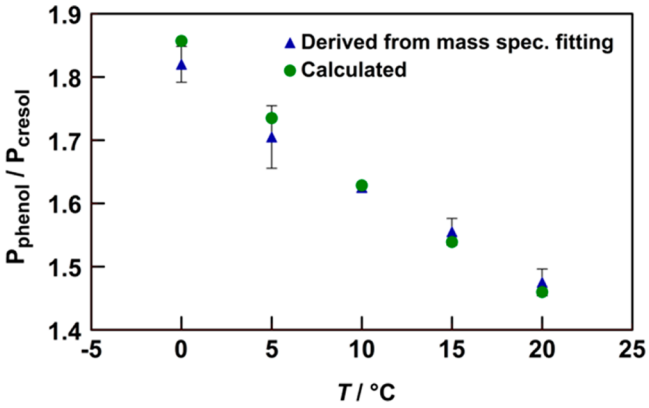

Figure 10. Partial pressure ratios in the vapor of a binary mixture of phenol and *o*-cresol that was held at various temperatures from 0 to 20 °C. Blue triangles are the ratios calculated by fitting mass spectra of the vapor collected for each temperature. Data for two identical experiments are averaged. Green dots are partial pressure ratios that are calculated for this ideal mixture. Error bars represent $\pm 1\sigma$, where σ is the standard deviation based on the two experiments.

Section 2. (Note that when comparing with partial pressure ratios, which are proportional to number density ratios, the $1/\sqrt{m}$ correction to flux that was mentioned in Section A is not used.) Within experimental error, the ratios derived from the mass spectral fitting methodology agree with the calculated ratios. There appears to be a slight systematic deviation at lower mixture temperatures, where the measured ratio is lower than the calculated ratio. This deviation may be explained by the preferential evaporation of the more volatile phenol during the course of the experiment. The experimental measurement accurately determines the partial pressure ratio of the vapor pressure of this binary solution and is even sensitive enough to detect changes in the composition of the mixture as one component evaporates preferentially over another. Thus, our analysis procedure appears to be a credible approach for determining relative mole fractions from mass spectral data. It should be noted, however, that this validation experiment used two compounds of similar molecular mass and therefore is not sensitive to a systematic error caused by setting the mass-dependent transmission function to a constant value.

4. DISCUSSION

Our results are consistent with the general description of three overlapping stages of pyrolysis as represented in Figure 2. Earlier results suggest that H_2O and phenol, as well as phenol's methyl substituted derivatives, are evolved in the first stage ($T \approx 200-550$ °C). We observe H_2O from 100 °C to nearly 700 °C, with the peak yield coming at a temperature of 350 °C (see Figure 8). The evolution of H_2O well below 300 °C is likely to be the result of the outgassing of H_2O that was simply absorbed by PICA, which is known to be hygroscopic. Note that no attempt was made to degas the samples (other than holding them in vacuum overnight) before they were subjected to heat. As the sample temperature approaches 300 °C, the desorption of absorbed H_2O should be complete and additional H_2O would be expected to be produced by condensation reactions. Ouchi and Honda[20] suggested that the evolution of water from a phenolic resin near 350 °C is the result of a condensation reaction that leads to the formation of a diphenyl ether cross-link between phenol groups, as illustrated in Figure 11. FTIR measurements collected by Trick and Saliba[22] on a carbon/

DOI: 10.1021/am507816f
ACS Appl. Mater. Interfaces 2015, 7, 1383−1395

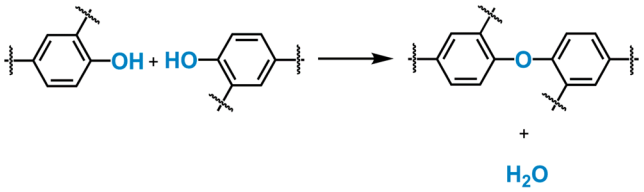

Figure 11. Condensation reaction between two adjacent hydroxyl groups to form a diphenyl ether group and H_2O. Based on a mechanism proposed by Ouchi and Honda[20] and Ouchi.[23]

phenolic composite corroborate the existence of a diphenyl ether group, as evidenced by an observed absorption at 1264 cm^{-1}. A small peak at m/z = 115 in our mass spectral data is also possible evidence that diphenyl ether is an intermediate in the pyrolysis of PICA (Figure 6). The m/z = 115 peak, which could be from a daughter fragment of diphenyl ether, begins to evolve at 250 °C, rises to a maximum at 350 °C, and becomes insignificant between 450 and 500 °C, which is consistent with the observations made by Ouchi and Honda. However, 2-methyl-napthalene is another possible minor product that has a daughter fragment at m/z = 115, but the structure of this molecule consists of two fused benzene rings and more closely resembles a product that would be expected from the char layer. It is generally accepted that the char layer consists of fused aromatic rings, and volatile products from the char layer are therefore expected to be observed at higher temperatures. Thus, if an unconsidered high-mass species is contributing to the signal at m/z = 115, diphenyl ether is the more likely possibility, but it will be necessary to extend the data to higher mass ranges to verify the production of this species.

Phenol and its methyl substituted derivatives are also liberated during the first pyrolysis stage ($T \approx 200-550$ °C). Our results show that higher-mass species, including phenol, cresol, and dimethyl phenol are observed from 250 to 450 °C, with a maximum at 350 °C. Parker and Winkler[21] proposed that aromatic groups that are part of the polymer backbone are retained and that only pendant aromatic groups are released as phenol and cresol (they did not discuss dimethyl phenol in this context, but one might imagine that it could also come from liberation of a pendant group), see Figure 12. Our results

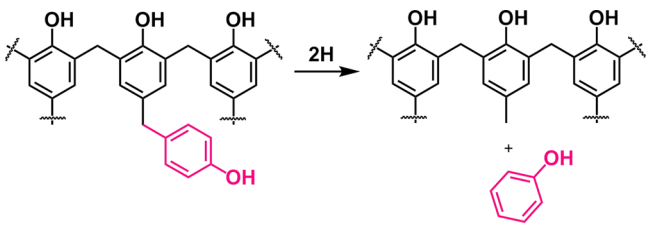

Figure 12. Liberation of a pendant group in the form of a phenol molecule. Based on the proposal by Parker and Winkler[21] that phenol (and presumably its substituted derivatives) can only be produced from pendant groups on the polymer backbone.

support this proposed decomposition pathway, as we observe phenol and its methylated derivatives over a narrow temperature range and in relatively small quantities. Xylene is also assigned in the mass spectra and appears in the same temperature range as phenol and its methyl substituted derivatives. The mechanism of xylene production has not been discussed previously, and its origin is unknown. In fact, the assignment of xylene as a product is still ambiguous (vide infra). If the assignment is correct, then the shift in maximum yield toward higher temperatures relative to phenol and its derivatives might indicate a transition in the pyrolysis mechanism where the evolution of oxidized aromatic species is giving way to less oxidized aromatic species that are still volatile.

CO_2 is also observed in the first pyrolysis stage but with relatively low yield (Figure 8). CO_2 reaches a maximum yield at 200 °C and stays relatively constant, with a slight dip at 250 °C, until 400 °C where it begins to drop. Jackson and Conley[18] suggested that CO_2 is evolved from the decomposition of carboxylic acid groups that are formed by the oxidation of methylol groups remaining after the resin has cured. This idea was supported by infrared spectra that revealed the presence of residual methylol functional groups even after curing at 120 °C. Postcuring in air would presumably lead to the oxidation of these methylol groups, and subsequent heating would release CO_2 (Figure 13).

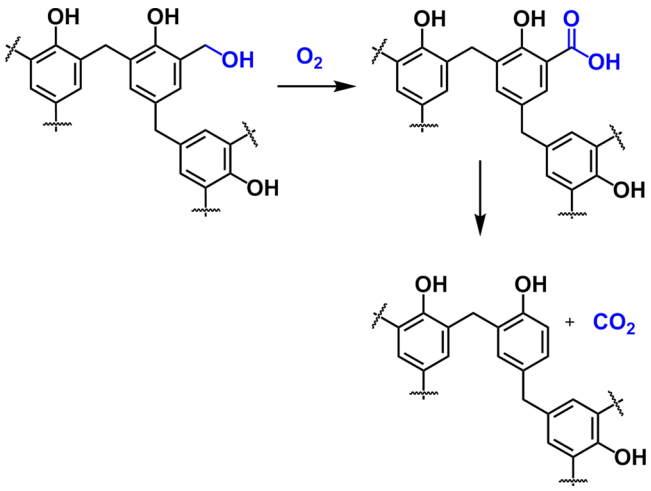

Figure 13. Oxidation of a methylol group leads to formation of a carboxylic acid group that subsequently decomposes and releases a CO_2 molecule. Based on a mechanism proposed by Jackson and Conley.[18]

The predominant pyrolysis product that we observed during the second stage of pyrolysis ($T \approx 400-800$ °C) was CO, which actually evolved over the entire experimental temperature range. Our results indicate that CO has a relatively low yield at temperatures below ~300 °C. Above 300 °C the CO yield rises steeply with temperature to a maximum at 450 °C, after which the yield drops quickly as the temperature increases to 600 °C and then only slowly decreases as the temperature increases further. Mechanisms proposed by Jackson and Conley[18] and by Ouchi[23] suggest that CO is produced as a result of the decomposition of a carbonyl cross-link in the polymer (Figure 14). The FTIR studies of Trick and Saliba[22] showed direct evidence for a carbonyl stretch at 1658 cm^{-1}, but the low intensity of the absorption did not support the decomposition of carbonyl cross-links as the main mechanism for the production of CO. The mass fragments collected in our experiment were limited to a range from m/z = 10 to 119, which did not enable the unique detection of a high-mass product containing a carbonyl cross-link. We do, however, observe a small peak at m/z = 105, which might be evidence for a larger, carbonyl-containing compound, such as benzophenone or 4-(methylphenyl)-phenyl-methanone. The main peak in the

DOI: 10.1021/am507816f
ACS Appl. Mater. Interfaces 2015, 7, 1383−1395

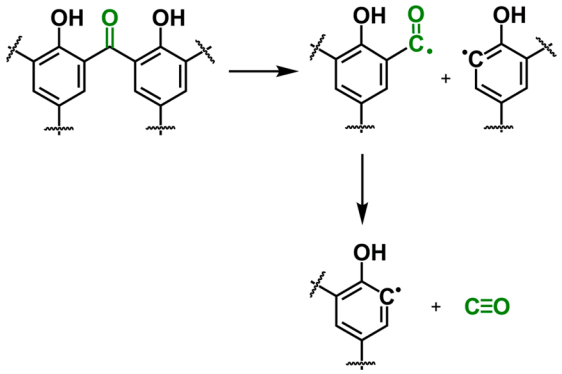

Figure 14. Two-step decomposition of a carbonyl cross-link to produce CO. The carbonyl cross-link may be the result of the oxidation of a methyl cross-link during the postcure of the phenolic resin in air. Based on similar mechanisms proposed by Jackson and Conley[18] and by Ouchi.[23]

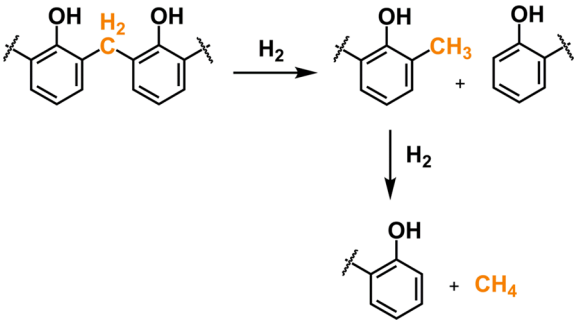

Figure 15. Two-step decomposition of a methylene bridge to produce CH_4. Based on a mechanism proposed by Ouchi.[23]

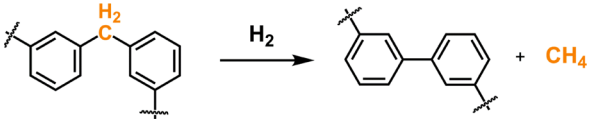

Figure 16. One-step decomposition of methylene bridge to produce CH_4. Based on a mechanism proposed by Trick and Saliba.[22]

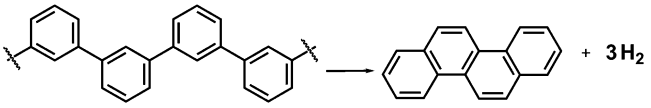

Figure 17. An unstable char coalesces to a stable char and H_2 is evolved. Based on a mechanism proposed by Trick and Saliba[22]

mass spectrum of benzophenone appears at m/z = 105, and 4-(methylphenyl)-phenyl-methanone has a significant daughter fragment at this m/z ratio. Benzophenone has a significant peak at m/z = 182, and 4-(methylphenyl)-phenyl-methanone has a significant peak at m/z = 196. The observation of peaks at either m/z = 182 or m/z = 196 in conjunction with the observed peak at m/z = 105 would give strong evidence for a carbonyl cross-link. Ouchi and Honda[20] also suggested that CO may be released from the decomposition of the diphenyl ether bonds created during the first stage of pyrolysis. The observation of H_2O during Stage 1 of the pyrolysis (see curve for H_2O in Figure 8) and the likely production of diphenyl ether bonds during this process (Figure 11) suggest that ether cross-link species might be involved in the production of CO. Unfortunately, we do not have any direct evidence for either proposed pathway to CO. Such evidence must wait for future experiments which cover a higher mass range of products. Under the assumption that carbonyl cross-links are the main source of CO, we suppose that these cross-links persist in low concentration even at relatively high temperatures, as CO continues to be evolved well above 600 °C. Without proof of carbonyl cross-links from mass spectra collected with a higher mass range, we have fit the m/z = 105 peak in our mass spectra with xylene, as mass spectra of the methylbenzene derivatives (e.g., xylene) also have peaks at m/z = 105. It is unsatisfactory at this point, however, that we cannot propose a chemical mechanism for the production of xylene. Thus, the curve associated with xylene in Figure 8 might actually arise from a daughter of a compound with a carbonyl functional group, which would imply that xylene is not actually a pyrolysis product.

CH_4 is another significant product that evolves during the second pyrolysis stage (Figure 8). Ouchi[23] proposed that CH_4 is the product of a two-step decomposition mechanism between methylene cross-links and H_2, followed by the thermal decomposition of the methyl functional groups that are produced (Figure 15). The first step in the reaction mechanism involves the reaction of hydrogen with the carbon cross-link to form a methyl substituted benzene ring and benzene. H_2 then reacts further with the methyl substituted aromatic ring to form methane. Alternatively, Trick and Saliba[22] propose that H_2 reacts with a methylene cross-link to form a single bond between the two aromatic groups, resulting in the evolution of methane (Figure 16). In both mechanisms, H_2 would presumably come from the fusing of aromatic rings (Figure 17), although one could imagine similar mechanisms to those shown in Figures 16 and 17, where breaking bonds create radical sites which abstract H atoms from nearby C−H moieties and H_2 is not an actual reactant. A variety of substituted aromatic molecules might possibly be evolved in addition to methane in the two-step mechanism proposed by Ouchi. We do observe substituted phenol products in the temperature range 300−450 °C. CH_4 is evolved at slightly higher temperatures, which is reasonable if the second step to produce CH_4 (Figure 15) requires more energy. Thus, our data are consistent with the proposed mechanism of Ouchi. We did not have the capability when we conducted our experiments to observe the high-mass polyphenyl products that would support the mechanism proposed by Trick and Saliba.

H_2 is expected to be the dominant pyrolysis gas as temperatures climb above 560 °C into the third stage of pyrolysis.[20,21] Although our mass spectrometer was not set up for detecting H_2 when we performed these experiments, we did detect its presence with a residual gas analyzer that was in the sample chamber. This observation supports the carbonization mechanism proposed by Ouchi and Honda[20] (Figure 17) and is in direct contrast to the mechanism proposed by Jackson and Conley,[18] in which H_2 is not evolved during the entire course of pyrolysis. Parker and Winkler[21] predicted the evolution of water and hydrogen at temperatures that approach 700 to 800 °C. Our quantitative data do not support this mechanism, as we do not observe water above 700 °C. Furthermore, GC studies by Sykes[26] and by Wong et al.[27] both detected H_2 as the dominant product when the pyrolysis temperature of a phenolic resin exceeded 480 °C.

B. Quantitative Yields of Pyrolysis Products. Quantitative yields of pyrolysis products of phenolic resins as a function

DOI: 10.1021/am507816f
ACS Appl. Mater. Interfaces 2015, 7, 1383−1395

of temperature have been measured by Sykes[26] and by Wong et al.,[27] who both used GC. GC can provide absolute measurements of the components of a gaseous or liquid mixture, but it has limitations for quantifying pyrolysis products because the products are not measured in situ. Instead, they are typically collected over a much longer time period (~1 h) than the 0.5–10 min data collection times used in our study, and then they are analyzed later by GC, often with multiple columns because of the broad range of volatilities of the pyrolysis products.

A comparison of our experimental results to the results obtained by Sykes[26] and later by Wong et al.[27] reveals similarities and differences between the relative product yields. First, it should be made clear that Sykes studied a novolac phenolic resin, Wong et al. studied a pure resole phenolic resin, and we studied the carbon/phenolic, PICA. All three studies reveal similar results with respect to the production of H_2O, which has the highest yield relative to other pyrolysis products during the first stage of pyrolysis. The data collected by Sykes suggested that H_2O desorption reaches a maximum at 450 °C. On the other hand, our data indicate that H_2O desorption has a maximum at 350 °C, which is close to the peak value of 374 °C obtained by Wong et al.

Sykes and Wong et al. reported a higher yield of CH_4 than CO over the temperature range of pyrolysis, while our results show the opposite trend. Ouchi and Honda[20] found a relationship between the quantity of oxygenated species evolved and the degree of hydroxyl substitution on the phenol molecules used in the synthesis of phenolic resins. Specifically, they discovered that higher degrees of hydroxyl substitution lead to higher yields of H_2O, CO, and CO_2 relative to the yield of CH_4. Ouchi also reported that the peak production of CO and CO_2 shifts to lower temperatures with an increase in hydroxyl substitution. In light of Ouchi's findings, our results suggest that the resin used in the fabrication of PICA might have a higher degree of hydroxyl functional group substitution than what is present in the parent phenol molecule. This result is difficult to confirm from the manufacturer because of the proprietary nature of the material. We also cannot confirm that the phenolic resin used by Sykes and by Wong et al. had a lower degree of hydroxyl group substitution because the details of the polymer were not reported.

Ouchi and Honda[20] also studied the relationship between methyl substitution and CH_4 production, and they found that a higher degree of methyl substitution on the phenol molecule leads to a shift in the peak production of CH_4 to lower temperatures. A similar result was found for the point at which CH_4 was first detected. Ouchi and Honda postulated that two different reactions account for the production of CH_4. First, any methyl groups that remain in the polymer after it has been synthesized are dissociated during the early stage of pyrolysis. Second, the cleavage of methylene cross-links and their subsequent reaction with any available hydrogen provides a source of CH_4 at higher temperatures. In the study performed by Ouchi and Honda, the temperature range for the detection of CH_4 from resins synthesized without methyl substituted phenol consistently spanned 300 to 850 °C, with peak CH_4 production between 580 and 600 °C. CH_4 was detected between 250 and 800 °C when they pyrolyzed two separate resins synthesized from *m*-cresol and 3,5-dimethyl phenol. CH_4 was detected with a peak in its production at 500 °C for both resins, suggesting that methyl substitution tends to facilitate the release of CH_4 at lower temperatures. Our results are similar to those that Ouchi and Honda observed with the methyl substituted resins. We observed CH_4 desorption over a range of temperatures that span 300 to 750 °C, with a maximum yield at 450 °C. We thus surmise that the phenol resin in PICA has significant methyl functional group substitution.

Sykes[26] reported the detection of higher molecular weight species in the form of phenol and 2,4-dimethyl phenol, with a maximum yield at 500 °C. Wong et al. did not report yields of phenol and its derivatives in their study. Our analysis shows that phenol, cresol, and dimethyl phenol have maximum yields at ~350 °C, which is shifted to lower temperatures relative to the data collected by Sykes. Sykes did not report the observation of xylene or any related derivatives, but Wong et al. reported maximum yields of benzene, toluene, and xylene at 527 °C. We did not observe toluene or benzene but did (possibly) observe xylene with a maximum yield at 400 °C. Our observation of substituted phenol/benzene derivatives with maximum yields at lower temperatures than those observed by Sykes and Wong et al., respectively, may be explained the higher degree of methyl and hydroxyl group substitution in PICA, as suggested above. Our results indicate that dimethyl phenol and cresol desorb with higher yields than phenol, which is further evidence that the phenol backbone in the resin in PICA has significant methyl substitution.

5. CONCLUSION

Relative molar yields of the main pyrolysis products from the carbon/phenolic ablator, PICA, with molecular masses from 10 to 119 amu, have been derived from in situ measurements in vacuum, with the use of a differentially pumped mass spectrometer detector. A fitting procedure for the analysis of mass spectra collected at approximately 50 °C intervals, spanning a temperature range from 100 to 935 °C, has been implemented in order to calculate the relative molar yields as a function of temperature. These yields are discussed in light of prior work on the pyrolysis of various phenolic resins and phenolic/carbon composites. A consistent qualitative description of the decomposition pathways that occur in three stages of pyrolysis covering the temperature range from ~200 °C to ~1000 °C has emerged, with light gases being produced in the highest yields at all stages. H_2O is the dominant product in the first stage, with some CO_2 also being formed. CO is the main product during the second stage, and CH_4 is also significant during this stage. H_2 becomes dominant in the third stage, as the production of CO decreases. The heavier products (e.g., phenol, its methylated derivatives, and possibly even heavier species) have relatively low yields and desorb mainly during the second stage. The quantitative yields are apparently strongly influenced by the exact molecular structure of the phenolic resin. A comparison of our results with those of earlier studies suggests that the phenolic resin used in PICA has significant hydroxyl and methyl substitution on the phenyl rings of the polymer. The relative molar yields and the general mechanistic understanding provided by this work should be directly applicable to emerging material response models that target PICA as a focus material. The in situ mass spectrometric method that has been described here is well suited for follow-on studies of the decomposition kinetics as a function of temperature under nonequilibrium conditions, with the potential to provide even more detailed data for increasingly sophisticated models that seek to describe the thermal behavior of practical carbon/phenolic heat shields such as PICA in an atmospheric entry environment.

DOI: 10.1021/am507816f
ACS Appl. Mater. Interfaces 2015, 7, 1383–1395

■ ASSOCIATED CONTENT

Supporting Information

Relative molar yields of 14 species that contributed significantly to the mass spectral data. This material is made available free of charge via the Internet at http://pubs.acs.org.

■ AUTHOR INFORMATION

Corresponding Author

*E-mail: tminton@montana.edu.

Notes

The authors declare no competing financial interest.

■ ACKNOWLEDGMENTS

This work was supported by the National Aeronautics and Space Administration (Grants NNX13AN06G and NNX14AH76G). The authors are grateful to Dr. Nagi N. Mansour for many helpful discussions.

■ REFERENCES

(1) Hankey, W. L. *Re-Entry Aerodynamics*. AIAA Education Series; Przemieniecki, J. S., Ed., AIAA: Washington, D.C., 1988.

(2) Diaconis, N. S.; Fanucci, J. B.; Sutton, G. W. The Heat Protection Potential of Several Ablation Materials for Satellite and Ballistic Re-Entry into the Earth's Atmosphere. *Planet. Space. Sci.* **1961**, *4*, 463−478 DOI: 10.1016/0032-0633(61)90152-0.

(3) Ungar, E. W. Ablation Thermal Protection Systems Suitability of Ablation Systems to Thermal Protection Depends on Complex Physical and Chemical Processes. *Science* **1967**, *158*, 740−744 DOI: 10.1126/science.158.3802.740.

(4) Johnson, S. M.; Gasch, M. J.; Leiser, D.; Stewart, D. Jr.; Stackpoole, M.; Thornton, J.; Espinoza, C. Development of New TPS at NASA Ames Research Center.. In *15th AIAA International Space Planes and Hypersonic Systems and Technologies Conference*; Dayton, OH, April 28−May 1, 2008 ; AIAA: Washington, D.C., 2008; DOI: 10.2514/6.2008-2560.

(5) Feldman, J.; Gasch, M. J.; Poteet., C. C.; Szalai, C. Advanced Rigid Ablative Thermal Protection Systems. In *50th AIAA Aerospace Sciences Meeting including the New Horizons Forum and Aerospace Exposition*; Nashville, TN, Jan 9−12, 2012 ; AIAA: Washington, D.C., 2012; DOI: 10.2514/6.2012-472.

(6) Venkatapathy, E.; Laub, B.; Hartman, G. J.; Arnold, J. O.; Wright, M. J.; Allen, G. A., Jr. Thermal Protection System Development, Testing, and Qualification for Atmospheric Probes and Sample Return Missions: Examples for Saturn, Titan and Stardust-Type Sample Return. *Adv. Space Res.* **2009**, *44*, 138−150 DOI: 10.1016/j.asr.2008.12.023.

(7) Titov, E. V.; Kumar, R.; Levin, D. A.; Anderson, B. P. Modeling the Crack Growth in the AVCOAT Heat Shield. *49th AIAA Aerospace Sciences Meeting including the New Horizons Forum and Aerospace Exposition*; Orlando, FL, Jan 4−7, 2011 ; AIAA: Washington, D.C., 2011; DOI: 10.2514-6.2011-137.

(8) Tran, H. K.; Johnson, C. E.; Rasky, D. J.; Hui, F. C. L.; Hsu, M.; Chen, Y. K. Phenolic Impregnated Carbon Ablators (PICA) for Discovery Class Missions. *31st AIAA Thermophysics Conference*; New Orleans, LA, June 17−20, 1996 ; AIAA: Washington, D.C., 1996; DOI: 10.2514/6.1996-1911.

(9) Beck, R. A. S.; Driver, D. M.; Wright, M. J.; Hwang, H. H.; Edquist, K. T.; Sepka, S. A. Development of the Mars Science Laboratory Heat Shield Thermal Protection System. *J. Spacecr. Rockets* **2014**, *51*, 1139−1150 DOI: 10.2514/1.A32635.

(10) Szalai, C.; Slimko, E.; Hoffman, P. Mars Science Laboratory Heat Shield Development, Implementation, and Lessons Learned. *J. Spacecr. Rockets* **2014**, *51*, 1167−1173 DOI: 10.2514/1.A32673.

(11) Trumble, K. A.; Cozmuta, I.; Sepka, S.; Jenniskens, P.; Winter, M. Postflight Aerothermal Analysis of Stardust Sample Return Capsule. *J. Spacecr. Rockets* **2010**, *47*, 765−774 DOI: 10.2514/1.41514.

(12) Bose, D.; White, T.; Santos, J. A.; Feldman, J.; Mahzari, M.; Olson, M.; Laub, B. Initial Assessment of Mars Science Laboratory Heat Shield Instrumentation and Flight Data. In *51st AIAA Aerospace Sciences Meeting including the New Horizons Forum and Aerospace Exposition*; Grapevine, TX, Jan 7−10, 2013 ; AIAA: Washington, D.C., 2013; DOI: 10.2514/6.201-908.

(13) Space X website, http://www.spacex.com/news/2013/02/09/spacexs-dragon-spacecraft-successfully-re-enters-orbit (accessed Nov 3, 2014).

(14) April, G. C.; Pike, R. W.; del Valle, E. G. Modeling Reacting Gas Flow in the Char Layer of an Ablator. *AIAA J.* **1971**, *9*, 1113−1119 DOI: 10.2514/3.6330.

(15) Kendal, R. M.; Bartlett, E. P.; Rindal, R. A.; Moyer, C. B. *An Analysis of the Coupled Chemically Reacting Boundary Layer and Charring Ablator: Part 1*. NASA CR-1060; NASA: Washington, D.C., 1968.

(16) Lachaud, J.; Cozmuta, I.; Mansour, N. N. Multiscale Approach to Ablation Modeling of Phenolic Impregnated Carbon Ablators. *J. Spacecr. Rockets* **2010**, *47*, 910−921 DOI: 10.2514/1.42681.

(17) Pilato, L. *Resin Chemistry. Phenolic Resins: A Century of Progress.*; Springer, New York, 2010; pp 41−45; DOI: 10.1007/978-3-642-04714-5.

(18) Jackson, W. M.; Conley, R. T. High Temperature Oxidative Degradation of Phenol−Formaldehyde Polycondensates. *J. Appl. Polym. Sci.* **1964**, *8*, 2163−219 DOI: 10.1002/app.1964.070080516.

(19) Morterra, C.; Low, M. J. D. IR Studies of Carbons-VII. The Pyrolysis of a Phenol-Formaldehyde Resin. *Carbon* **1985**, *23*, 525−530 DOI: 10.1016/0008-6223(85)90088-0.

(20) Ouchi, K.; Honda, H. Pyrolysis of Coal 1. Thermal Cracking of Phenol-Formaldehyde Resins Taken as Coal Models. *Fuel* **1959**, *38*, 429−443 DOI: 10.1021/la00063a010.

(21) Parker, J. A.; Winkler, E. L. *The Effects of Molecular Structure on the Thermochemical Properties of Phenolics and Related Polymers*. NASA TR R-276; NASA: Washington, D.C., November 1967.

(22) Trick, K. A.; Saliba, T. A. Mechanisms of the Pyrolysis of Phenolic Resin in a Carbon/Phenolic Composite. *Carbon* **1995**, *33*, 1509−1515 DOI: 10.1016/0008-6223(95)00092-R.

(23) Ouchi, K. Infra-Red Study of Structural Changes During the Pyrolysis of a Phenol-Formaldehyde Resin. *Carbon* **1966**, *4*, 59−66 DOI: 10.1016/0008-6223(66)90009-1.

(24) Friedman, H. L. Products of Flash Pyrolysis of Phenol-Formaldehyde by Time-of-Flight Mass Spectroscopy. *J. Appl. Polym. Sci.* **1965**, *9*, 651−662 DOI: 10.1002/app. 1965.070090225.

(25) Shulman, G. P.; Lochte, H. W. Thermal Degradation of Polymers. II. Mass Spectrometric Thermal Analysis of Phenol-Formaldehyde Polycondensates. *J. Appl. Polym. Sci.* **1966**, *10*, 619−635 DOI: 10.1002/app.1966.070100407.

(26) Sykes, G. F. *Decomposition Characteristics of a Char-Forming Phenolic Polymer Used For Ablative Composites*; NASA TN D-3810; NASA: Washington, D.C., February 1967.

(27) Wong, H. W.; Peck, J.; Edwards, R.; Reinisch, G.; Lachaud, J.; and Mansour, N. N. Measurement of Pyrolysis Products from Phenolic Polymer Thermal Decomposition. *AIAA Science and Technology Forum and Exposition*; National Harbor, MD, January 2014; AIAA: Washington, D.C., 2014; DOI: 10.2514/6.2014-1388.

(28) Sobera, M.; Hepter, J. Pyrolysis-Gas Chromatography-Mass Spectrometry of Cured Phenolic Resins. *J. Chromat. A* **2003**, *993*, 131−135 DOI: 10.1016/S0021-9673(03)003881-1.

(29) Bennett, A.; Payne, D. R.; Court, R. W. Pyrolytic and Elemental Analysis of Decomposition Products from a Phenolic Resin. *Macromol. Symp.* **2014**, *339*, 38−47 DOI: 10.1002/masy.201300136.

(30) Zhang, J.; Garton, D. J.; Minton, T. K. Reactive and Inelastic Scattering Dynamics of Hyperthermal Oxygen Atoms on a Saturated Hydrocarbon Surface. *J. Chem. Phys.* **2002**, *117*, 6239−6251 DOI: 10.1063/1.1460858.

(31) Garton, D. J.; Brunsvold, A. L.; Minton, T. K.; Troya, D.; Maiti, B.; Schatz, G. Experimental and Theoretical Investigations of the Inelastic and Reactive Scattering Dynamics of O (^{3}P) + D_2. *J. Phys. Chem. A* **2006**, *10*, 1327−1341 DOI: 10.1021/jp054053k.

DOI: 10.1021/am507816f
ACS Appl. Mater. Interfaces 2015, 7, 1383−1395

(32) Lee, Y. T.; McDonald, J. D.; LeBreton, P. R.; Herschbach, D. R. Molecular Beam Reactive Scattering Apparatus with Electron Bombardment Detector. *Rev. Sci. Instrum.* **1969**, *40*, 1402−1408 DOI: 10.1063/1.1683809.
(33) Alexander, W. A.; Wiens, J. P.; Minton, T. K.; Nathanson, G. M. Reactions of Solvated Electrons Initiated by Sodium Atom Ionization at the Vacuum-Liquid Interface. *Science* **2012**, *35*, 1072−1075 DOI: 10.1126/science.1215956.
(34) Stein, S. E. Mass Spectra. In *NIST Chemistry WebBook*, NIST Standard Reference Database Number 69; Linstrom, P. J., Mallard, W. G., Eds.; National Institute of Standards and Technology: Gaithersburg, MD; http://webbook.nist.gov (accessed August 2, 2014).
(35) Deverse, F. T.; King, A. B. Effect of Molecular Structure on the Ionization Probabilities of Aromatic Molecules. *J. Chem. Phys.* **1964**, *41*, 3833−3838 DOI: 10.1063/1.1725822.
(36) Harrison, A. G.; Jones, E. G.; Gupta, S. K.; Nagy, G. P. Total Cross Sections for Ionization by Electron Impact. *Can. J. Chem.* **1966**, *44*, 1967−1973 DOI: 10.1021/ie50480a054.
(37) Hudson, J. E.; Hamilton, M. L.; Vallance, C.; Harland, P. W. Absolute Electron Impact Ionization Cross-Sections for the C_1 to C_4 Alcohols. *Phys. Chem. Chem. Phys.* **2003**, *5*, 3162−3168 DOI: 10.1039/b304456d.
(38) Kim, Y. K., Irikura, K. K., Rudd, M. E., Ali, M. A., Stone, P. M., Chang, J., Coursey, J. S., Dragoset, R. A., Kishore, A. R., Olsen, K. J., Sansonetti, A. M., Wiersma, G. G., Zucker, D. S., Zucker, M. A. *Electron-Impact Ionization Cross Section for Ionization and Excitation Database* (version 3.0, 2004). Available: http://physics.nist.gov/ionxsec (accessed August 2, 2014).
(39) Rhodes, F. H.; Wells, J. H.; Murray, G. W. Vapor Composition Relationships in the Systems Phenol−Water and Phenol−Cresol. *Ind. Eng. Chem.* **1925**, *17*, 1199−1201 DOI: 10.1021/ie50191a044.
(40) Biddiscombe, D. P.; Martin, J. F. Vapor Pressures of Phenol and the Cresols. *Trans. Faraday Soc.* **1958**, *54*, 1316−1322 DOI: 10.1039/TF9585401316.

DOI: 10.1021/am507816f
ACS Appl. Mater. Interfaces 2015, 7, 1383−1395